Journal of Alloys and Compounds 504S (2010) S332–S335

Contents lists available at ScienceDirect

Journal of Alloys and Compounds

journal homepage: www.elsevier.com/locate/jallcom

Crystallization of colloidal amorphous precursor particles into $BaFe_{12}O_{19}$ with hexagonal structure by aerosol annealing process

Hye Moon Lee [a,*], Yong-Jin Kim [a], Jung-Ho Ahn [b]

[a] Functional Materials Division, Korea Institute of Materials Science, 531 Changwondaero, Changwon Gyeongnam 641-831, South Korea
[b] Faculty of Engineering, Andong National University, Songchun-dong, Andong, Gyungbuk 760-749, South Korea

ARTICLE INFO

Article history:
Received 31 July 2009
Received in revised form 4 March 2010
Accepted 9 March 2010
Available online 15 March 2010

Keywords:
Barium ferrite
Fine particles
Aerosol annealing process
Phase transformation
Magnetic properties

ABSTRACT

Aerosol annealing process was firstly applied to the phase transformation of barium ferrite ($BaFe_{12}O_{19}$) precursor particles from amorphous phase to hexagonal structure. The aerosol annealing process was experimentally optimized by the control of annealing temperature and particle residence time in the hot zone. By a proper control of aerosol annealing process, the crystallized $BaFe_{12}O_{19}$ particles with a geometric mean diameter (D_p) of 174 nm, a geometric standard deviation (σ_g) of 1.21, and an intrinsic coercivity (H_{ci}) of 3336 Oe were successfully prepared.

1. Introduction

Barium ferrite ($BaFe_{12}O_{19}$) fine particle with hexagonal structure is one of the interesting candidate materials for the preparation of high-density magnetic recording media due to their fairly large magnetocrystalline anisotropy, high Curie temperature, large saturation magnetization and coercivity, and excellent chemical stability and corrosion resistivity [1–3].

Chemical liquid phase method is very useful for the synthesis of a mono- or poly-dispersed metal, oxide, or semiconductor nanoparticles [4]. $BaFe_{12}O_{19}$ precursor particles with diameters of ~5 nm with good monodispersity have been fabricated by a sodium citrate-aided process [5]. For the application of $BaFe_{12}O_{19}$ precursor particles synthesized by the liquid phase method to magnetic recording media, it is necessary to transform amorphous phase to hexagonal structures. Kim et al. [5] have employed a post-annealing process at temperatures higher than 600 °C for the phase transformation, resulting in successful preparation of $BaFe_{12}O_{19}$ particles with hexagonal structure. However, the prepared particles were over-sintered because the high temperature annealing process was performed in the state of all precursor particles which were put in an alumina boat. The sintered $BaFe_{12}O_{19}$ particles had to be further ball-milled to refine to nanosize, resulting in irregular powder morphology.

An aerosol annealing process is very effective against particle agglomeration occurred in the phase transformation because the annealing process is performed in the state of precursor particles which are dispersed in gas. Lee et al. [6] have examined an electrospray pyrolysis, one of aerosol annealing processes, to prepare chemically ordered $L1_0$ FePt nanoparticles. Unsintered spherical $L1_0$ FePt nanoparticles were successfully prepared by the aerosol process, but the annealing process performed at oxygen free environment pyrolytically converted the organics, surrounding non-oxide particles, into lots of carbon particles. It is thus expected that the aerosol annealing process is more adequate for the preparation of oxides than non-oxide particles because the organics, such as surfactants and solvents, can be completely burnt out by the annealing process performed even in air.

The purpose of this study was to develop a continuous synthesis method of spherical $BaFe_{12}O_{19}$ fine particles, avoiding an excessive sintering during the post-annealing process. In this study, we have first tried to attempt an aerosol annealing process for the preparation of unsintered spherical $BaFe_{12}O_{19}$ fine particles with hexagonal phase particles from amorphous phase to hexagonal structure.

2. Experimental

The $BaFe_{12}O_{19}$ amorphous colloidal suspension was synthesized by a sodium citrate-aided method using $Fe(NO_3)_3 \cdot 9H_2O$ (Aldrich; ≥99%), $BaCl_2 \cdot 2H_2O$ (Aldrich; ≥99%), and $Na_3C_6H_5O_7 \cdot 2H_2O$ (Aldrich; ≥99%) in the presence of sodium hydroxide. The molar ratio of Ba^{2+}/Fe^{3+}/citrate was fixed at 1:12:13. The total concentration of

* Corresponding author. Tel.: +82 55 280 3519; fax: +82 55 280 3392.
E-mail address: hyelee@kims.re.kr (H.M. Lee).

0925-8388/$ – see front matter © 2010 Elsevier B.V. All rights reserved.
doi:10.1016/j.jallcom.2010.03.100

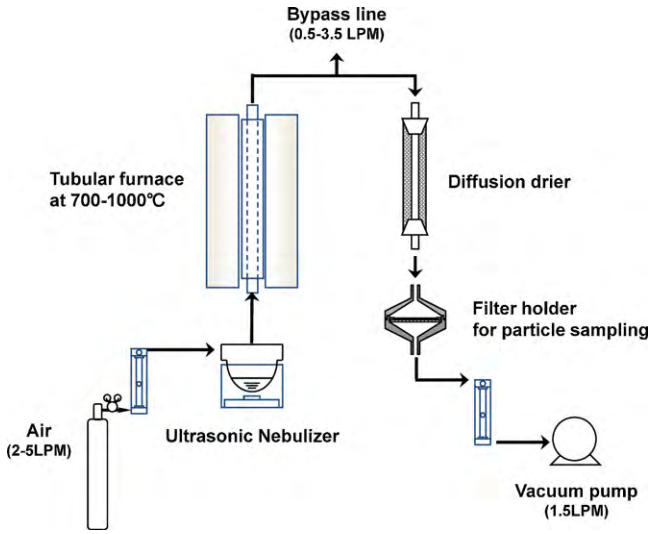

Fig. 1. Schematic diagram of aerosol annealing system for phase transformation of barium ferrite amorphous particles.

$BaCl_2$ (0.027 M) is kept constant in this study. The detailed preparation method is previously described [5].

Fig. 1 shows the aerosol annealing system used for the phase transformation of $BaFe_{12}O_{19}$ precursor particles produced by the sodium citrate-aided method. The precursor $BaFe_{12}O_{19}$ colloidal suspension was nebulized by a nebulizer with an ultrasonic wave of 1.72 MHz. Air, at a flow rate of 2–5 l/min, was used to carry the nebulized droplets with $BaFe_{12}O_{19}$ precursor particles into the quartz tube (length of 500 mm and inner diameter of 10 mm) heated by an electric furnace at 700–1000 °C. The precursor particles remained during 0.11–0.36 s in the hot zone. The gas leaving the tubular furnace contained both $BaFe_{12}O_{19}$ particles and water vapors. The evaporated water was removed by a diffusion drier since the solvent vapors enhance aerosol particle agglomeration [7]. And finally, the prepared dry spherical $BaFe_{12}O_{19}$ particles were collected on a membrane filter.

Crystal structure analyses for the prepared particles were performed using an X-ray diffractometer (XRD; Rigaku D/Max 2200) with Cu Kα radiation. The morphologies of the particles were observed by a transmission electron microscopy (TEM; JEOL, JEM-2100F) and a scanning electron microscopy (SEM; JEOL, JSM-5800). A vibrating sample magnetometer (VSM; Lakeshore, 7400S) was used for analyzing the magnetic properties of the prepared $BaFe_{12}O_{19}$ particles at room temperature, with a maximum field of 10 kOe.

3. Results and discussion

Fig. 2(a) and (b) show a TEM image of the $BaFe_{12}O_{19}$ precursor particles synthesized by the sodium citrate-aided method on a carbon coated TEM grid and XRD patterns of the precursor and annealed particles, respectively. The precursor particles have a quite uniform shape with a narrow size distribution. The mean particle diameter (D_p) was ~3 nm with a geometric standard deviation (σ_g) of ~1.1. XRD pattern for the precursor particles showed an amorphous phase, but the $BaFe_{12}O_{19}$ hexagonal phase was clearly observed in the XRD pattern for the particles annealed at 800 °C for 100 min. This suggests that the sodium citrate-aided method permits the production of homogenous $BaFe_{12}O_{19}$ precursor nanoparticles of about 3 nm.

To find an optimized temperature for the phase transformation of $BaFe_{12}O_{19}$ precursor particles from amorphous to hexagonal structure, $BaFe_{12}O_{19}$ particles were prepared by heating the nebulized precursor particles at the aerosol annealing temperatures of 700–1000 °C with a carrier gas flow rate of 2 LPM. The resulting crystal structure and magnetic property analyses were examined. Fig. 3(a) shows XRD patterns of particles annealed at 700, 750, 800, 850, 900, 950, and 1000 °C, respectively. The particles prepared at 700–800 °C showed amorphous phase in their XRD patterns, but it was clearly observed that $BaFe_{12}O_{19}$ hexagonal phase starts to appear in the particles annealed at 850 °C. Kim et al. [5] experimentally showed that $BaFe_{12}O_{19}$ precursor particles started to be transformed into hexagonal phase at ≥600 °C. The difference between their results and ours could be explained by processing heating time of precursor particles in the hot zone. Although the precursor particles were annealed at relatively low temperatures in Kim et al.'s study, their processing time (100 min) in the hot zone was enough to transform the precursor particles into hexagonal phases. However, the precursor particle residence time in our process was extremely short (0.271 s), so that the higher temperature than Kim et al.'s should be necessary to let the precursor particles absorb enough thermal energy for their phase transformation. Fig. 3(b) shows magnetic hysteresis loops, indicating intrinsic coercivity, H_{ci}, remanent magnetization, M_r, and saturation magnetization, M_s, for the $BaFe_{12}O_{19}$ precursor particles and the aerosol annealed at 800, 850, 900, 950, and 1000 °C, respectively. H_{ci}, M_r and M_s sharply increased from 20 to 2988 Oe, 0 to 19 emu/g and 14 to 35 emu/g, respectively, as the annealing temperature increased up to 900 °C. As shown in the XRD patterns of Fig. 3(a), the crystallinity of $BaFe_{12}O_{19}$ hexagonal phase was clearly improved as the annealing temperature increased up to 900 °C. This indicates that the sudden increase of magnetic properties was caused by the enhanced $BaFe_{12}O_{19}$ hexagonal structure. When the annealing temperature increased from 900 to 1000 °C, however, H_{ci}, M_r and M_s smoothly and gradually increased from 2988 to 3321 Oe, 19 to 26 emu/g, and 35 to 44 emu/g, respectively. Cabanas et al. [8] experimentally showed that crystallinity and crystallite size of $BaFe_{12}O_{19}$ particles have a significant effect on their magnetic properties. Although the XRD patterns for the specimens prepared

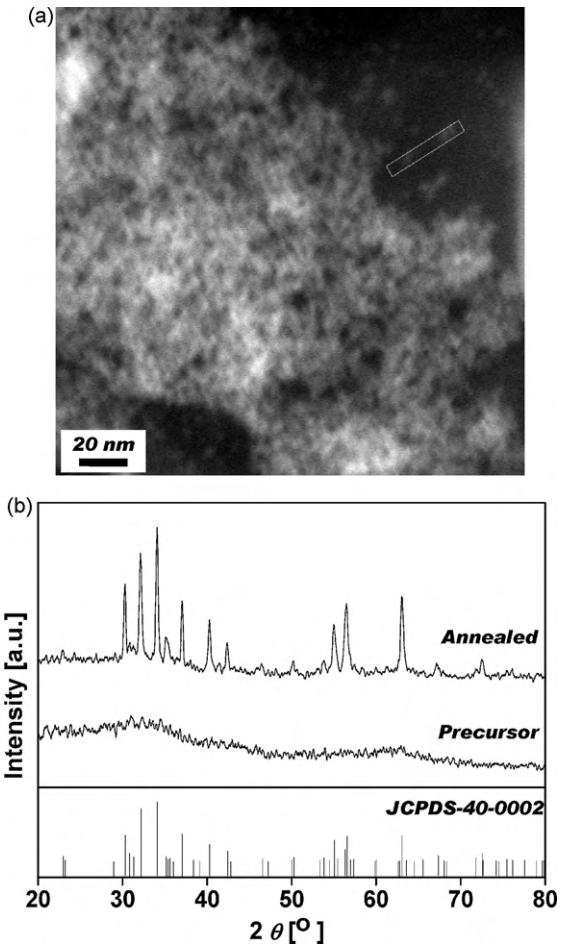

Fig. 2. TEM image of the precursor particles (a) and XRD patterns of barium ferrite particles as-synthesized and annealed at 800 °C (b).

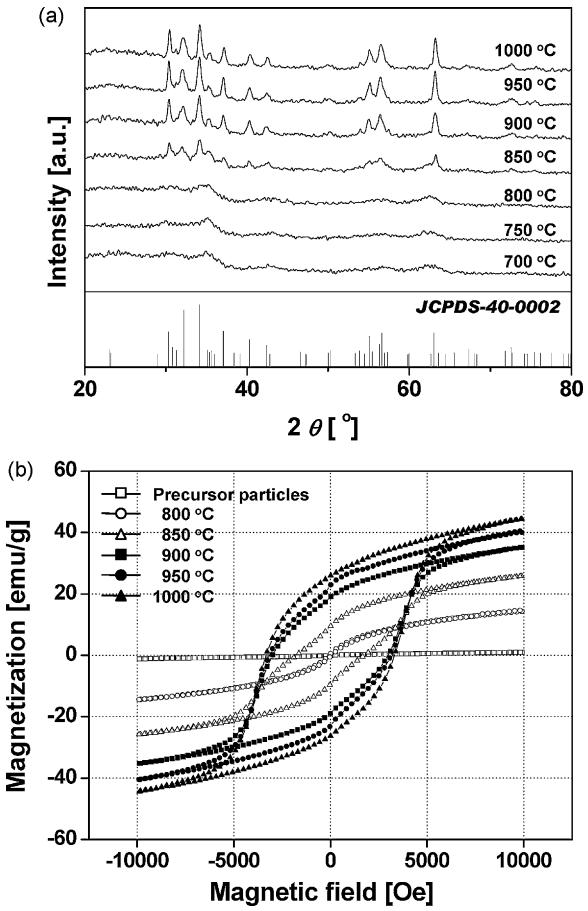

Fig. 3. XRD patterns (a) and magnetic hysteresis loops (b) for barium ferrite particle annealed at 700, 750, 800, 850, 900, 950, and 1000 °C.

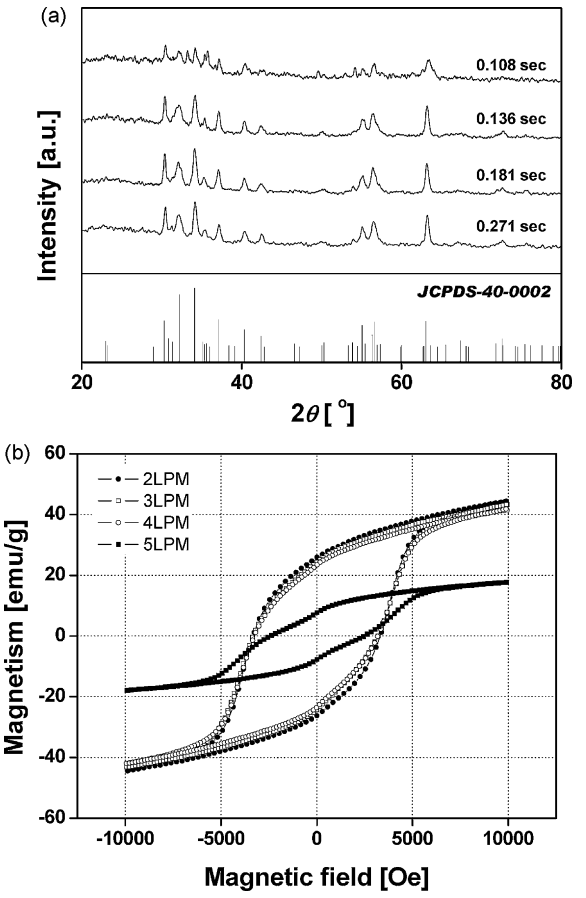

Fig. 4. XRD patterns (a) and magnetic hysteresis loops (b) for barium ferrite particle annealed for 0.108, 0.136, 0.181, and 0.271 s.

at 900 and 950 °C showed clear crystal structures of $BaFe_{12}O_{19}$ hexagonal phase, this is often the case even when there is small amounts of amorphous phase in the prepared particles. The hysteresis loops for the $BaFe_{12}O_{19}$ particles annealed at 900, 950, and 1000 °C seemed to be characteristic of a superparamagnetic material. However, some anomalies were observed in the loops annealed at 900 and 950 °C, indicating small amounts of amorphous phase in the particles prepared at 900 and 950 °C. In addition, the crystallite sizes of $BaFe_{12}O_{19}$ particles prepared at 900, 950, and 1000 °C were also calculated by Scherrer's equation. It is noticed that the use of Scherrer's equation is not for determining an accurate crystallite size but for investigating the effects of temperature on the increase of crystallite size for particles prepared by the aerosol annealing process. The calculated crystallite sizes for the normalized intensity of (1 1 4) plane were 16, 17, and 18 nm for the particles annealed at 900, 950, and 1000 °C, respectively, and those of (2 2 0) plane were 16, 24, 25 nm. The results showed that the causes for the gradual improvement of magnetic properties were both slight increases of crystallinity and crystal sizes with increasing the aerosol annealing temperature.

Fig. 4(a) and (b) show XRD patterns and magnetic hysteresis loops for the $BaFe_{12}O_{19}$ particles annealed at carrier gas flow rates of 2, 3, 4, and 5 LPM (residence time of 0.271, 0.181, 0.136, and 0.108 s, respectively), respectively. The XRD patterns for all the prepared particles showed $BaFe_{12}O_{19}$ hexagonal structure. On the other hand, the normalized pattern intensity for the prepared at 5 LPM was much lower than those for the prepared at 2, 3, and 4 LPM. In addition, an anomaly was clearly observed in the magnetic hysteresis loop for the $BaFe_{12}O_{19}$ particles prepared at 5 LPM, so that their magnetic properties (H_{ci}: 2415 Oe, M_r: 8 emu/g, M_s: 18 emu/g) were much lower than those (H_{ci}: 3192–3336 Oe, M_r: 23–26 emu/g, and M_s: 42–45 emu/g) for the particles annealed at 2, 3, and 4 LPM. These indicate that the residence time of the nebulized droplets with $BaFe_{12}O_{19}$ precursor particles was too short to fully transform their crystal phase into hexagonal structure as the carrier gas flow rate was 5 LPM. Accordingly, it could be known that equal to or longer residence time than 0.136 s is the desirable for transforming the $BaFe_{12}O_{19}$ precursor particles into hexagonal structure in the aerosol annealing system.

The SEM images and size distributions of $BaFe_{12}O_{19}$ particles annealed for 0.108 s (5 LPM), 0.136 s (4 LPM), 0.181 s (3 LPM), and 0.271 s (2 LPM) are shown in Fig. 5. Particle diameter was determined by measuring more than 300 particles for each sample in the SEM images of prepared $BaFe_{12}O_{19}$ particles. As shown in the SEM images, it was clearly observed that all the prepared barium ferrite particles were unsintered and spherical in their morphology. As mentioned earlier, this is because the aerosol annealing process was performed in the state of precursor particles which were dispersed in gas. The D_p for the $BaFe_{12}O_{19}$ particles decreased with the particle residence time in the hot zone. According to Okuyama and Lenggoro [9], carrier gas flow rate (i.e., residence time of heating or solvent evaporation) and temperature are the major parameters, which affect the morphology of particles generated by spray pyrolysis, as shown the aerosol annealing method in this study. Wang et al. [10] reported that the decrease of the nebulized droplet evaporation rate was the main reason for increasing the particle size in the spray pyrolysis process. In other words, as carrier gas flow rate increases (i.e., decrease of particle residence time in the hot zone), the evaporation rate of nebulized droplet with $BaFe_{12}O_{19}$ amor-

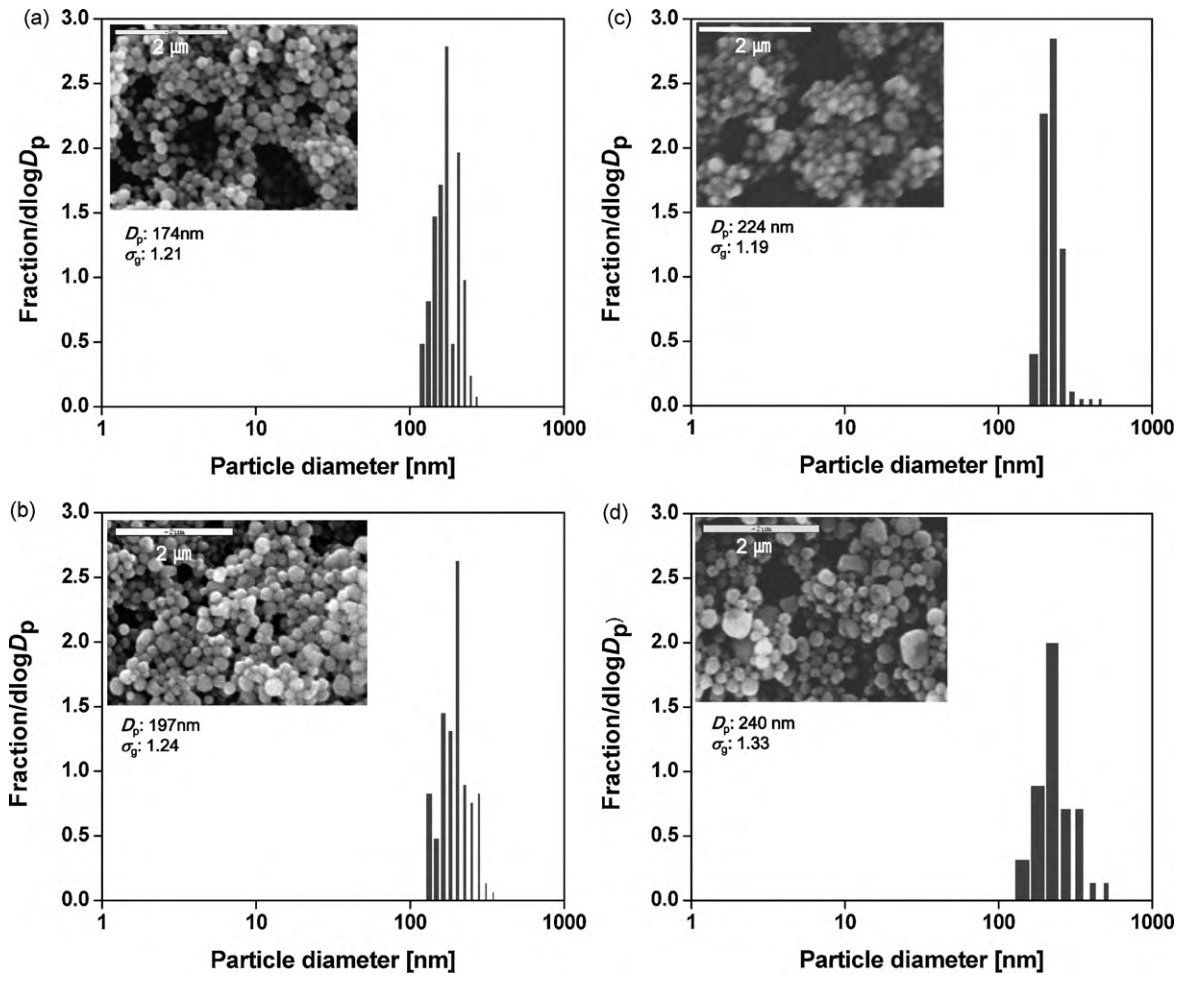

Fig. 5. SEM images and size distributions for the barium ferrite particles annealed for 0.271 s (a), 0.181 s (b), 0.136 s (c), and 0.108 s (d).

phous particles decreases, so that the particle size became smaller in this study.

Consequently, it could be known that the aerosol annealing process is applicable to the preparation of unsintered spherical $BaFe_{12}O_{19}$ fine particles with crystal structure of hexagonal phase and particle diameter of smaller than ~200 nm. For more effective application of the aerosol annealing process to the phase transformation of $BaFe_{12}O_{19}$ precursor particles into hexagonal structure, it is desirable to adjust the annealing temperature and particle residence time as equal to or higher than 1000 °C and equal to or longer than 0.136 s.

4. Conclusions

An aerosol annealing method was applied to the phase transformation of amorphous barium ferrite precursor particles, to hexagonal structure. Although the temperature for phase transformation was higher than the previous results, the aerosol annealing process was very effective in the continuous preparation of unsintered spherical barium ferrite fine particles. In order to apply the aerosol annealing method to the successful phase transformation of barium ferrite amorphous particles, the annealing temperature and particle residence time in hot zone should be adjusted to ≥1000 °C and ≥0.136 s, respectively. By a proper control of aerosol annealing method, nano-sized barium ferrite particles were successfully prepared.

Acknowledgement

This work was supported by a grant from Korea Institute of Materials Science, a subsidiary branch of Korea Institute of Machinery and Materials.

References

[1] H.-F. Yu, H.-Y. Lin, JMMM 283 (2004) 190.
[2] L. Fu, X. Liu, Y. Zhang, V.P. Dravid, C.A. Mirkin, Nanoletters 3 (2003) 757.
[3] X.H. Liu, M.H. Hong, W.D. Song, G.X. Chen, H.M.J. Lam, J.P. Wang, T.C. Chong, Appl. Phys. A 80 (2005) 611.
[4] J. Park, E. Lee, N.-M. Hwang, M. Kang, S.C. Kim, Y. Hwang, J.-G. Park, H.-J. Noh, J.-Y. Kim, T. Hyeon, Angew. Chem. Ind. Ed. 44 (2005) 2872.
[5] S.G. Kim, W.-N. Wang, T. Iwaki, A. Yabuki, K. Okuyama, J. Phys. Chem. C 111 (2007) 10175.
[6] H.M. Lee, S.G. Kim, I. Matsui, T. Iwaki, F. Iskandar, I.W. Lenggoro, K. Okuyama, JMMM 313 (2007) 62.
[7] H.M. Lee, K. Okuyama, A. Mizohata, T.-O. Kim, H. Koyama, Aerosol Sci. Technol. 41 (2007) 284.
[8] M.V. Cabanas, J.M. Gonzalez-Calbet, M. Labeau, P. Mollard, M. Pernet, M. Vallet-Regi, J. Solid State Chem. 101 (1992) 265.
[9] K. Okuyama, I.W. Lenggoro, Chem. Eng. Sci. 58 (2003) 537.
[10] W.-N. Wang, I.W. Lenggoro, K. Okuyama, J. Am. Ceram. Soc. 89 (2006) 888.